Robotics and Computer Integrated Manufacturing 57 (2019) 412–421

Contents lists available at ScienceDirect

Robotics and Computer Integrated Manufacturing

journal homepage: www.elsevier.com/locate/rcim

Design of cooperative mobile robots for co-manipulation and transportation tasks

B. Hichri*,[a], J-C. Fauroux[b], L. Adouane[b], I. Doroftei[c], Y. Mezouar[b]

[a] Luxembourg University, Luxembourg
[b] Institut Pascal, SIGMA Clermont, CNRS, Université Clermont Auvergne, ClermontFerrand F-63000, France
[c] "Gheorghe Asachi" Technical University of Iasi, Romania

ARTICLE INFO

Keywords:
Cooperative mobile robots
Design of lifting mechanisms
Object manipulation and transportation

ABSTRACT

This paper presents a design methodology for creating cooperative robots capable to manipulate and transport payloads. The strategy is based on tightening a payload between a set of mobile robots called m-bots. A lifting mechanism with two degrees of freedom mounted on each mobile robot allows then to lift the payload and put it on each m-bot top platform to be transported. Structural and dimensional analysis are detailed in order to develop the proposed mechanism. 3D multi-body dynamic software simulation results using different actuation for the lifting mechanism are presented. Experiments based on a developed test-bench and manufactured prototypes allow to validate the lifting process of the payload.

1. Introduction

The growing sector of logistics requires specifically designed machines and could highly benefit from robotics. Some logistics solutions require heavy infrastructure such as ground landmarks or guiding rails for Automated Guided Vehicles (AGVs) [1] or specific stacked storage racks as for Automated Storage and Retrieval System (ASRS). Human assistance could also be needed to put the object on the transporting platform (*e.g.,* for scissors elevators [2]). Forklifts [3] use forks to lift and transport the object but require to store the object on a pallet. Grabbing systems such as robot hands [4] limit the manipulated payload size and shape. Considering Manual transportation, many researches in the domain of Manual Material Handling (MMH) prove that operators have a better performance and less body suffering when keeping the payload low and close to the body [5–8]. According to the previous mentioned systems and to the previous studies linked to MMH, one can conclude that for a better stability, an object should be better transported on the robot body [9,10] or as close as possible to the robot body. Using this approach, it can be ensured to keep the gravity center above the polygon of support. Keeping the gravity center as low as possible also ensures a better stability margin on slopes.

A group of Robots working together for a task achievement presents several advantages compared to a single robot with a complex kinematics, such as a reduced cost, robustness, efficiency and improved performance [11–13]. Particularly for manipulation and transportation tasks, many collaborative robotic systems could be found in literature. Using different techniques, a group of similar [14,15] or heterogeneous robots [16] can ensure payloads transportation. Different strategies can be found in literature for multi-robot transportation. Pushing strategy proposed in [15] was used while a payload is on the ground. This strategy may face some difficulties depending on the friction generated by the contact surface with the ground and it can also affect the quality of the transported object. Other robots are using grabbing tools [17] for transportation which limits the shape of the objects that can be manipulated and requires geometries and shapes that could be gripped by the grippers. Some robots need the human assistance for putting payload on their transport platform such as the Arnold robot presented in [14]. In the proposed work, a strategy based on tightening a payload by a multi-robot system to manipulate it, lift it and autonomously put it on the robots platform autonomously is proposed. For our system we have supposed to use a mobile robot on which a manipulation mechanism is going to be mounted. The proposed solution will not be limited to a simple object category but will have to lift and transport objects of any shape and dimensions.

To ensure object lifting, a mechanism has to be chosen to ensure the movement of the object from an initial position on the ground to a final position on the robot body. For a better adaptability, a terminal organ ensuring a contact surface with the payload is used and the use of grippers is avoided because it limits the object shapes that can be manipulated and it also requires more actuators. To lift the object from the

* Corresponding author.
E-mail address: bassem.hichri@uni.lu (B. Hichri).

https://doi.org/10.1016/j.rcim.2019.01.002
Received 21 March 2018; Received in revised form 2 January 2019; Accepted 2 January 2019
Available online 07 January 2019

ground with a constant orientation, a variety of mechanisms that can ensure this function with different trajectories will be investigated. This general architecture allows to ensure the payload stability by putting it on the robot body. So a structural and dimensional synthesis for this mechanism are required to avoid collision problems and to ensure a better stability of the whole mechanism.

In this paper, a design strategy and implementation of cooperative robots for co-manipulation and transport of payloads of any shape and mass is proposed. Each robotic unit, called mono-robot or m-bot, is particularly characterized by its mechanical structure simplicity comparing to [9] and [18]. The resulting poly-robot, or p-bot, obtained by combining several m-bots around the payload, has the advantages of modularity while using a swarm of elementary robots [15,16], adaptability to objects of any shape and mass and ability to provide a fully autonomous system, without human mediation, contrary for example to the robotic system proposed in [19] or [20].

This paper is organized as follows. Section 2 presents the paradigm and requirements of the poly-robot, as well a the structural synthesis of the lifting mechanism on each mono-robot. Section 3 is dedicated to the dimensional synthesis and design of manipulation mechanism. Section 4 presents the simulation and experimental results. Finally, Section 5 presents a conclusion and targeted future works.

2. C^{3}bots paradigm

2.1. Specification

The Collaborative Cross and Carry Mobile Robots (C^{3}Bots) project aims to design identical mobile robots called **m-bots** equipped with a manipulation mechanism. The proposed work deals with collaborative tasks in which a group of similar entities are able to cooperate in order to achieve the task. It is dedicated to payloads of any shape co-manipulation and transport. The group of m-bots will be able to lift, co-manipulate and transport a payload which has to be laid on the top platform of each m-bot. Consequently, in addition to an end-effector, the m-bot manipulator has to include a lifting mechanism. The formed poly-robot, that we call **p-bot** (m-bot + payload), is characterized by its reconfigurability depending on the overall system stability and the success of task achievement. The set of robots configuration is obtained according to the positioning algorithm developed in [21,22] to ensure stability of the overall system (payload + m-bots) during the different task steps: co-manipulation and lifting, transportation and putting down the payload. The reconfigurabilty is needed to ensure the modification of the formation of the set of robots depending on the participant number of m-bots and in case of one or multiple robots break down. This reconfigurabilty is needed to allow the maintain of p-bot stability with respect to Static Stability Margin **SSM** and Force Closure Grasping **FCG** developed in [21,22]. The former is a criterion that ensures the stability during transportation phase and the latter ensures stability during manipulation phase. The m-bots architecture allows also the p-bot to maneuver in any direction and this is guaranteed by developing a centralized controller based on Virtual Structure **(VS)** Navigation developed in [22]. This controller ensures the control of each entity in a way that the set of robots evolve in a specified direction or have the same ICR to ensure coordinated rotation without loss of stability.

The general architecture of a m-bot is defined by the following requirements R_i presented in Table 1 and relative to the environment in which it will operate.

For simplicity reasons, the end-effector is considered here to be a rigid contact plate in order to fit variable payload contact surfaces. According to the previous requirements, the global co-manipulation method will be described.

Table 1
M-bot requirements.

Requirement	Definition
R_1	Lift a payload in collaboration with similar m-bots using a manipulation mechanism
R_2	Transport a payload.
R_3	Collision-free payload trajectory from the ground to the robot top platform with constant orientation.
R_4	Evolve in structured terrain.
R_5	Ensure manoeuvrability.
R_6	Ensure stability.
R_7	Ensure reconfigurability.
R_8	Tighten the contact payload/m-bot.
R_9	Detect other m-bots.
R_{10}	Detect obstacles.

2.2. Co-manipulation method

For a better stability of the payload and to avoid the risk of payload slipping and falling down between the m-bots end-effectors, the strategy of Army Ants transportation [10] was adopted for putting the payload on the m-bots top platform. Finally the co-manipulation and transportation method was decided and illustrated in Fig. 1.

The process of co-manipulation and transportation of a payload was initially described in [21,23,24]. The different phases of payload prehension, lifting and transportation are presented in Fig. 1. The first phase consists in locating the payload and surrounding it using distance

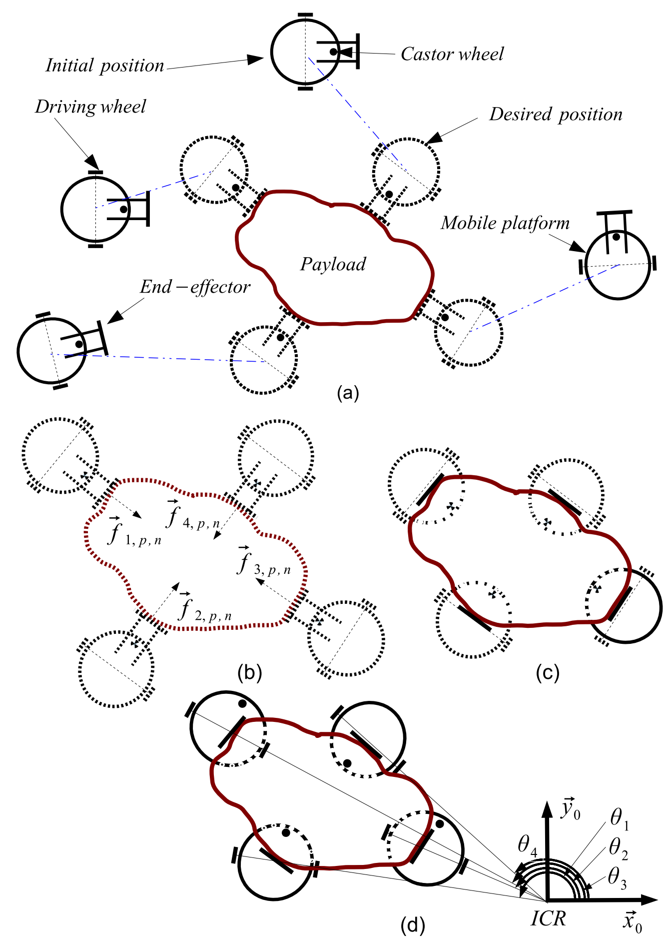

Fig. 1. Co-manipulation method: a) Target reaching; b) Object holding; c) Object set on robot bodies; d) Object transport: a unique Instantaneous Center of Rotation (ICR) requires different steering angles θ_m.

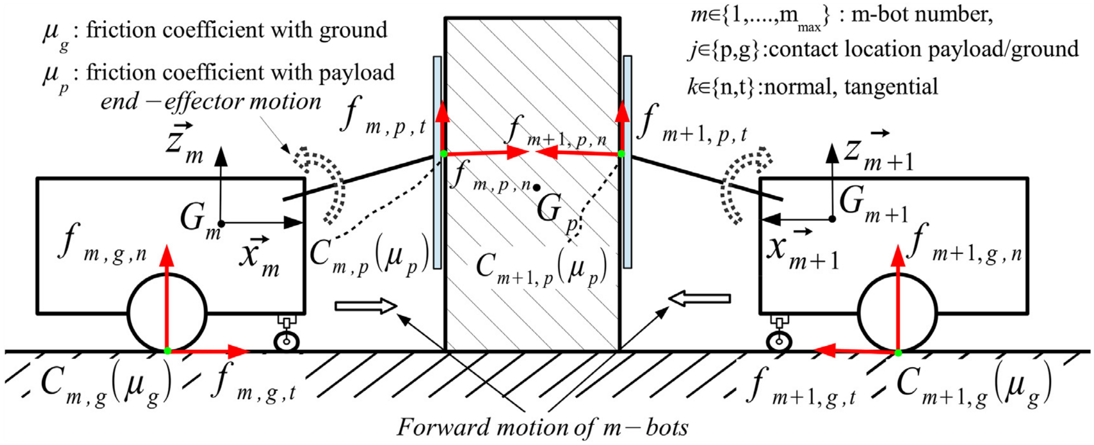

Fig. 2. Payload lifting by two m-bots.

sensors. The m-bots have to be oriented toward the object in order to face it (cf. Fig. 1(a)). Secondly, the payload is held by the m-bots end-effectors which exert a collective pressure using wheel propulsion (Fig. 1(b)). Submitted to collective pressure and to the proposed co-lifting manipulation, the object is elevated and laid on the m-bots top platforms (Fig. 1(c)). Finally, locomotion and transportation tasks are performed where each m-bot # m is steering by a suitable angle θ_m to ensure to the p-bot a unique Instantaneous Center of Rotation (ICR) (Fig. 1(d)).

2.3. Pre-dimensioning the lifting capacity

The forces applied to a m-bot are represented in Fig. 2 and denoted with a triple index $f_{m,\ j,\ k}$, with m the m-bot number, j the nature of the contact (g for ground, p for payload) and k the component of the force (n for normal, t for tangential).

A m-bot # m, with a mass M, could apply a pushing force $f_{m,\ p,\ n}$ at the contact point $C_{m,\ p}$ on the payload with a friction coefficient μ_p, which generates a lifting force $f_{m,\ p,\ t}$ counting on wheel propulsion. The contact point $C_{m,\ g}$ (wheel/gound) is characterized by a friction coefficient μ_g. The maximal lifting force for the m-bot # m can be written as:

$$f_{m,p,t} = \mu_p f_{m,p,n} = \mu_p f_{m,g,t} = \mu_p(\mu_g f_{m,g,n}) = \mu_p(\mu_g Mg) \tag{1}$$

The maximal total lifting force is

$$f_{p,t} = \sum_{m=1}^{m_{max}} f_{m,p,t} = m_{max}\mu_p(\mu_g Mg) \tag{2}$$

With the simplifying assumption $\mu_g = \mu_p = 0.5 \Rightarrow f_{p,t} = \frac{Mm_{max}g}{4}$. One can conclude that to increase the p-bot lifting capacity $f_{p,\ t}$, the total number m_{max} of m-bots, their mass M or the friction coefficients μ_g and μ_p have to be increased. As the environment and payload may be of different materials, the μ_g and μ_p coefficients are not precisely known and may be variable. They can be maximized by using adherent materials on the wheels and contact plate.

3. Designing a lifting mechanism

3.1. Specification of the lifting mechanism

The lifting and manipulation mechanism used for object lifting must ensure the following requirements R_{li} presented in Table 2:

Table 2
Manipulation mechanism requirements.

Requirement	Definition
R_{l1}	Manipulate payload via an end-effector.
R_{l2}	Allow object lifting.
R_{l3}	Ensure fittability on the robot mobile platform.
R_{l4}	Avoid collision with robot platform and the ground.
R_{l5}	Tighten contact payload/mechanism using the end-effector.
R_{l6}	Ensure fittability of the robot to the payload.
R_{l7}	Ensure orientability of the robot platform with respect to the payload.
R_{l8}	Put the payload on the robot body.

3.2. Structural and dimensional synthesis of the lifting mechanism

Structural selection

The various requirements R_i (cf. Table 1) and R_{li} (cf. Table 2) will influence directly the system kinematics structure. R_5 and R_{l7} can be satisfied by supporting the lifting mechanism on a turret. As a consequence, a revolute joint with z axis will support the mechanism (cf. Fig. 3(b), (c) and (d)). R_3 defines the initial and final poses P_1 and P_2 of the lower point P (cf. Fig. 5) of the end-effector that holds the object. The latter will keep its orientation constant during the lifting motion (R_3, R_{l1}). R_{l2} imposes that the trajectory starts with a vertical lifting motion ($+z_m$) and R_{l8} suggests that it finishes with a landing motion including a backward horizontal (-x_m) and a landing component ($-\ z_m$) towards the m-bot platform (Fig. 3(a)). R_3 and R_{l4} imply not to start the horizontal motion too early in order to avoid collision with the m-bot platform. Different trajectories are allowed (Fig. 3(a)) among which the square and the circular motions are the most obvious. A square trajectory could be achieved using two orthogonal prismatic joints and two actuators (Fig. 3(b)). A complex trajectory could also be ensured by using a cam mechanism with two slots (Fig. 3(d)) but the payload orientation would not be very precise. A circular trajectory would lead to a simpler solution using only one actuated revolute joint. However, to keep the payload orientation along the circular trajectory, a parallelogram mechanism is preferred (Fig. 3(c)) and keeps the control simplicity thanks to its single actuator. The proposed mechanism will be fixed on the top of a single axle mobile platform.

Structural analysis

Fig. 4 describes the proposed lifting mechanism. A turntable (Part *2*) is connected to the base (Part *1* fixed on the mobile platform) via a revolute joint (z_m axis) which allows the mobile platform of the robot to steer freely when the payload is on robot bodies (laid on surface S_2 on the top of *2*). Two identical parallelogram mechanisms are mounted on the turntable *2*. Each one is composed of a lower bar *3*, two long bars *4* and an end-effector support *5, 6, 7*. The payload to be manipulated is hold by the contact surface S_1 of the end-effector. An actuator *8* is used to ensure object lifting and to control the parallelogram mechanism via an additional lever *9*. The actuator allows to maintain the pressure force on the payload.

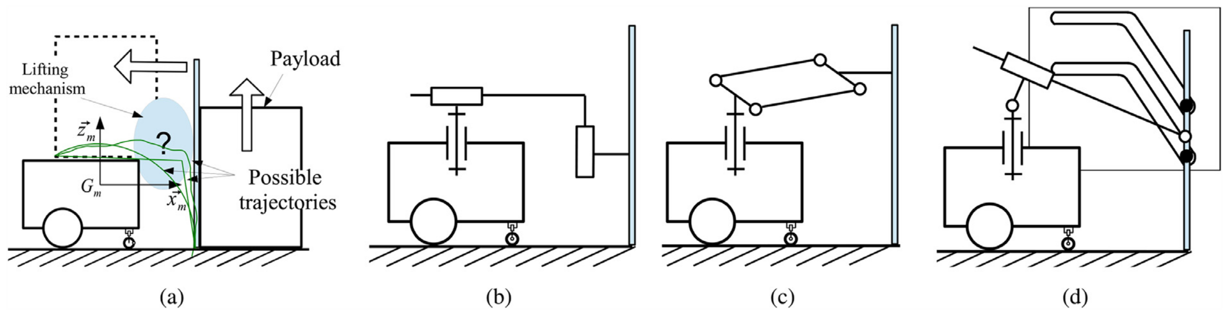

Fig. 3. Elementary lifting systems: a) Payload initial and final position with possible trajectories; b) 2 DOF solution; c) 1 DOF solution based on parallelogram mechanism; d) 1 DOF solution based on cam mechanism.

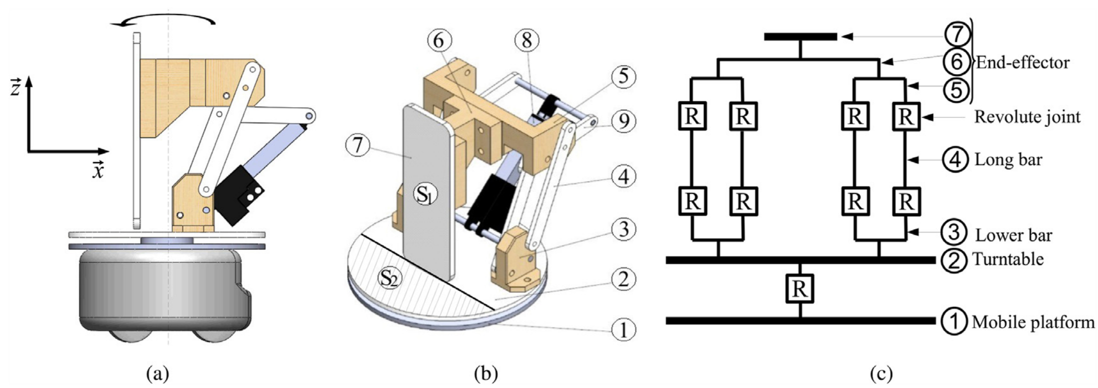

Fig. 4. Elementary lifting systems: a) 3D CAD for a m-bot [25]; b) 3D CAD view for the manipulation mechaism; c) Binding graph.

Dimensional synthesis

Trajectory radius determination

In order to define the parallelogram mechanism parameters, it is crucial to define:

- P_1: the initial contact point between the robot and the payload still on the ground;
- P_2: the arrival position of the payload on the robot platform (this position ensures to keep the m-bot platform stable);
- P_3: intermediate position defined by the clearances δ_1 and δ_2 to avoid collision between the robot end-effector and the mobile platform.

To calculate the trajectory radius (which corresponds to the long bars length *AB* and *PCD* that we denote *r*) the method consists in calculating the distances *a* and *b* (cf. Fig. 6) and solving the following second order equation:

$$r^2 = (h + r\sin\alpha_0)^2 + (a + b)^2. \tag{3}$$

The first step is to identify the constant *a* by using geometrical relations into right angle triangles which gives:

$$a = \frac{(l + \delta_1)^2 + (\delta_2)^2}{2(l + \delta_1)}. \tag{4}$$

The second step is to find the constant *b* by using geometrical relations into right angle triangles that gives:

$$b = \frac{\delta_2(h + r\sin\alpha_0)}{l + \delta_1}. \tag{5}$$

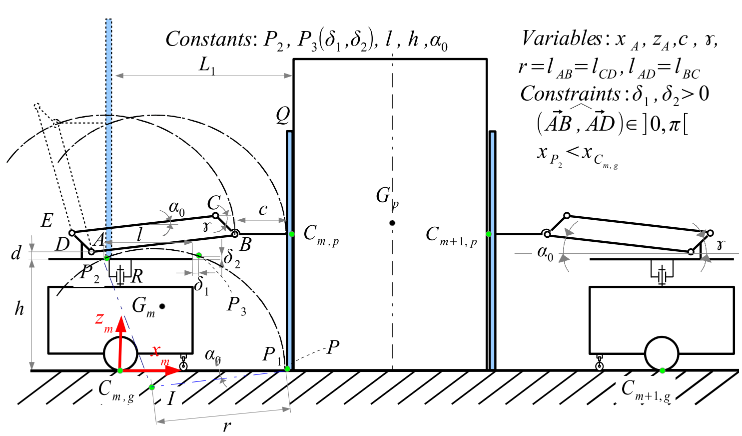

Fig. 5. Dimensions synthesis.

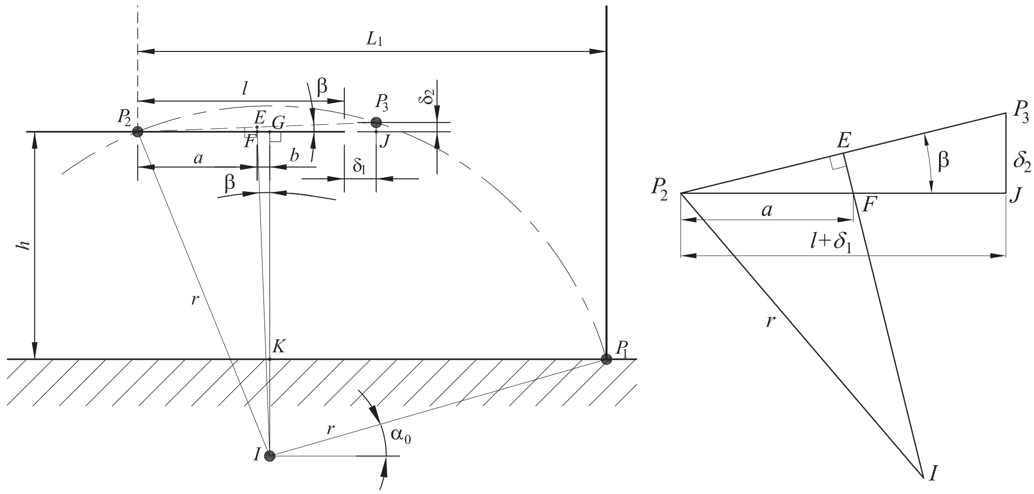

Fig. 6. Determination of the trajectory center *I*.

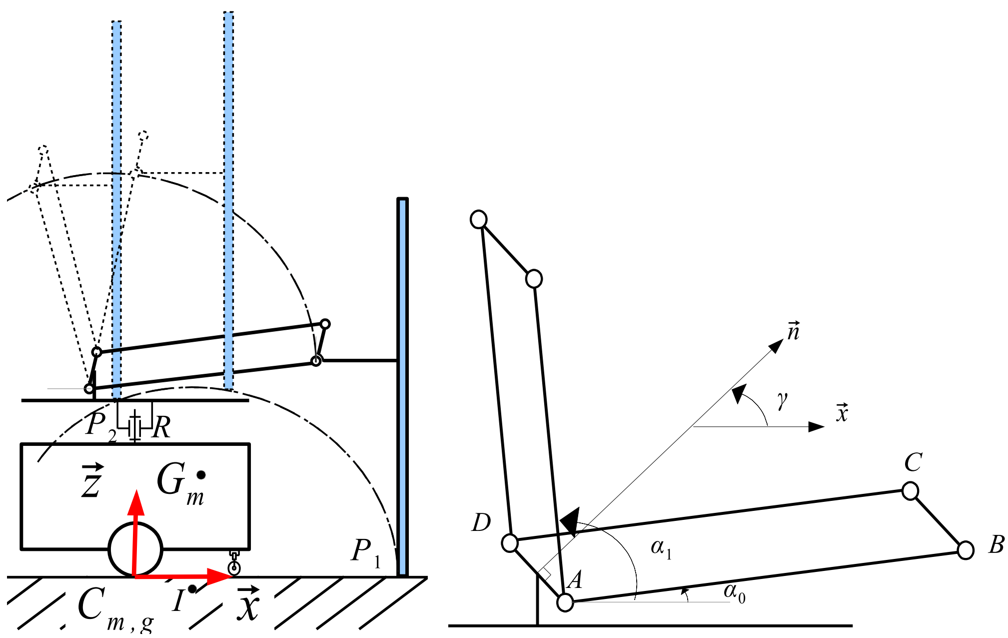

(a) (b)

Fig. 7. Extreme positions of the parallelogram mechanism.

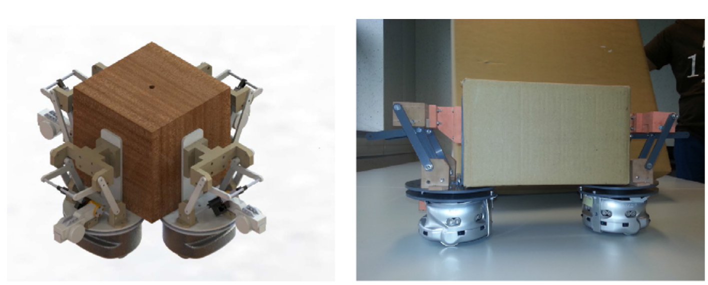

(a) 3D CAD (b) Manufactured prototypes

Fig. 8. Proposed design of the p-bot and manufactured system.

Now that the constant term $(a + b)$ of Eq. (3) is identified, the equation can be reformulated into a second order equation of unknown r. Solving (3) means to solve the following equation:

$$mr^2 + nr + p = 0 \tag{6}$$

with

$$m = -\frac{[(l+\delta_1)^2 + \delta_2^2](\delta_2 + 2h)\sin\alpha_0}{(l+\delta_1)^2};$$

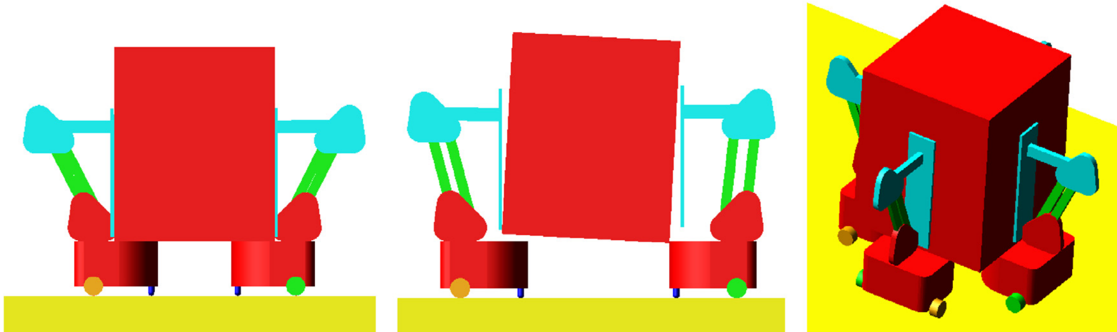

(a) (b) (c)

Fig. 9. Payload lifting using a passive mechanism: a) two m-bots successfully lifting; b) two m-bots failing to lift a payload; c) four m-bots supporting a payload.

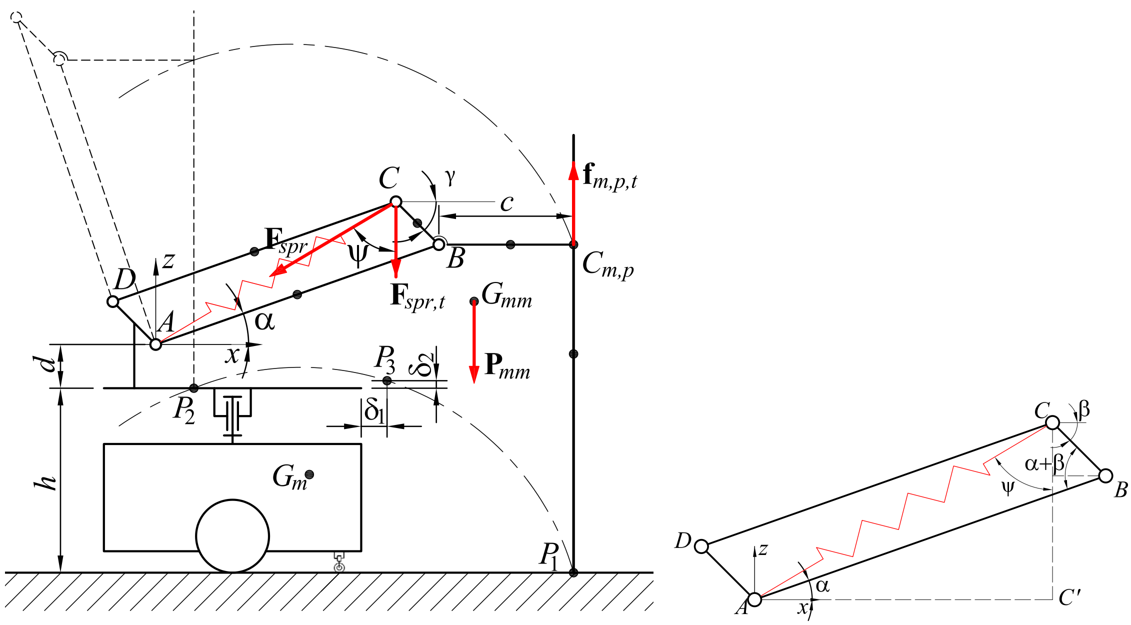

(a) (b)

Fig. 10. Payload lifting using a traction spring.

$$n = \frac{(l+\delta_1)^2\cos^2\alpha_0 - \delta_2^2\sin^2\alpha_0}{(l+\delta_1)^2};$$

$$p = \frac{[(l+\delta_1)^2+\delta_2^2][(l+\delta_1)^2+\delta_2^2+4h(\delta_2+h)]}{4(l+\delta_1)^2}$$

Finally r is equal to:

$$r = l_{AB} = l_{CD} = \frac{-m+\sqrt{m^2-4np}}{2n} \tag{7}$$

The distance between P_1 and P_2 can be deduced in function of constant parameters as follows

$$L_1 = A + r\cos\alpha_0 \tag{8}$$

with

$$A = \frac{(l+\delta_1)^2+(\delta_2)^2+2\delta_2(h+r\sin\alpha_0)}{2(l+\delta_1)}$$

$$x_{P_1} = x_{P_2} + L_1;\ \ z_{P_1} = 0 \tag{9}$$

Now the position of A and B can be written as:

$$x_A = x_{P_1} - r\cos\alpha_0 - c = x_{P_2} + A - c \tag{10}$$

$$z_A = h + d = z_{P_2} + d \tag{11}$$

$$x_B = x_A + r\cos\alpha_0 \tag{12}$$

$$z_B = z_A + r\sin\alpha_0 \tag{13}$$

Singular positions

To avoid singular positions of the parallelogram mechanism, $\widehat{BAD}$ must satisfy a constraint along the travel between α_0 and α_1 which is:

$$\widehat{BAD} \in \,]0, \pi[\tag{14}$$

When this constraint is satisfied along the trajectory between initial and final positions, the parallelogram mechanism would never have a flattened configuration as presented in Fig. 7(a). This constraint implies a suitable choice of γ angle, the angle of the normal vector $\vec{n}$ to segment AB with respect to horizontal.

From Fig. 7(b) one can conclude that, to avoid the parallelogram flattening, γ must be less than $\pi - \alpha_1$ and while considering always $\alpha_0 > 0$:

$$\gamma = \frac{\alpha_0+\alpha_1}{2} \in [0, \pi-\alpha_1] \tag{15}$$

where α_0 and α_1 are the extreme angular positions of the link AB.

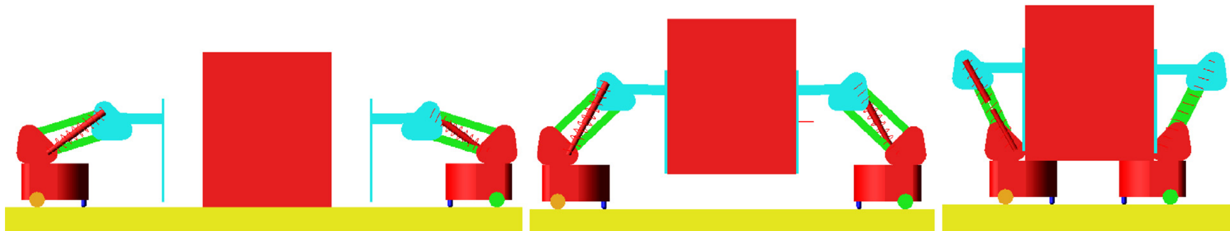

(a) Successful lifting of the payload.

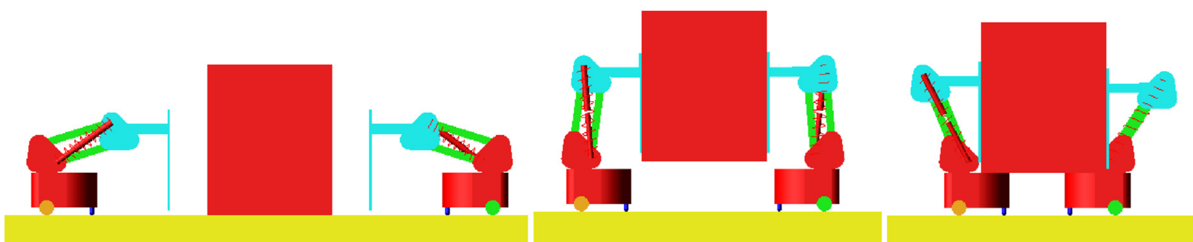

(b) Payload lifting with a low stiffness helical spring: the payload is able to slip because the generated tightening force is not sufficient to maintain it.

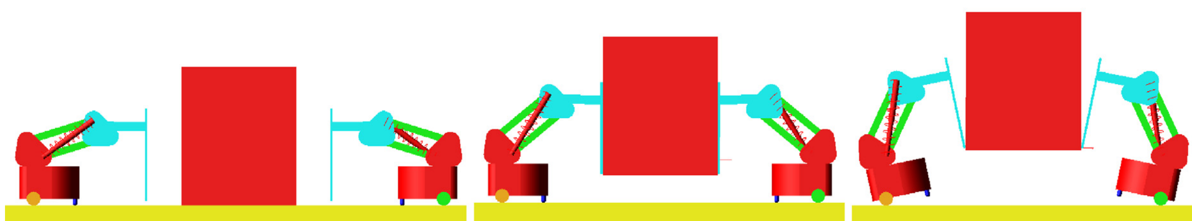

(c) The m-bots tip over when the deformation of used springs generate normal forces that exceeds the pushing forces generated by the robot's wheels propulsion.

Fig. 11. Multi-body dynamic simulation for payload lifting using helical extension springs.

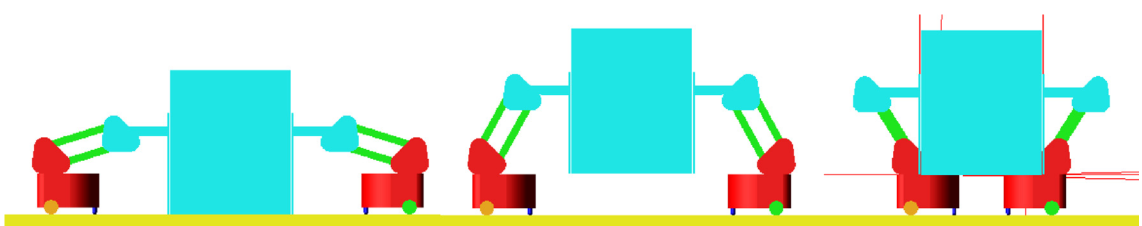

Fig. 12. Payload lifting using an interconnection system and actuated parallelogram system.

4. Mechanical simulations and experimental results

In order to validate our proposal for the co-manipulation and lifting strategy using a multiple robot system for payloads transportation, a multi-body dynamic simulation software was used in addition to an experimental test-bench. Simulation and experimental results are presented in following subsections. Fig. 8 presents the designed 3D CAD of the proposed system and two real prototypes for future experiments.

4.1. Multi-body dynamic system results

The simulation results were based on real physical parameters which were defined as follows:

- static friction coefficient end-effector/payload (rubber/steel), $\mu_p = 0.65$;
- static friction coefficient wheel/ground (rubber/asphalt), $\mu_g = 0.8$;
- m-bot mass, $M = 1.4$ kg. A constant torque was imposed on the m-bot wheels in order to impose the mobile platform propulsion and ensure the contact between the robots end effectors and the payload. The different cases previously studied in chapter 3 are illustrated and validated in the next subsections.

4.1.1. P-bot simulation for payload lifting

P-bot simulation using passive lifting mechanism. Fig. 9 shows the simulation results for a p-bot lifting a payload in order to put it on the top platform of its m-bots. Fig. 9(a) presents the successful task of lifting a payload of a limited mass with high friction contact between the payload and the end-effector. Contrary to the previous simulation, a higher payload mass produce a loss of stability with a decreasing applied tightening force with the variation of inclination angle of the parallelogram linkages (Fig. 9(b)). Fig. 9(c) presents a successful limited payload mass lifting while using four m-bots. The system is able to lift a payload with a mass around 0.2 kg with two m-bots (Fig. 9(a)) and around 0.4 kg with four m-bots (Fig. 9(c)).

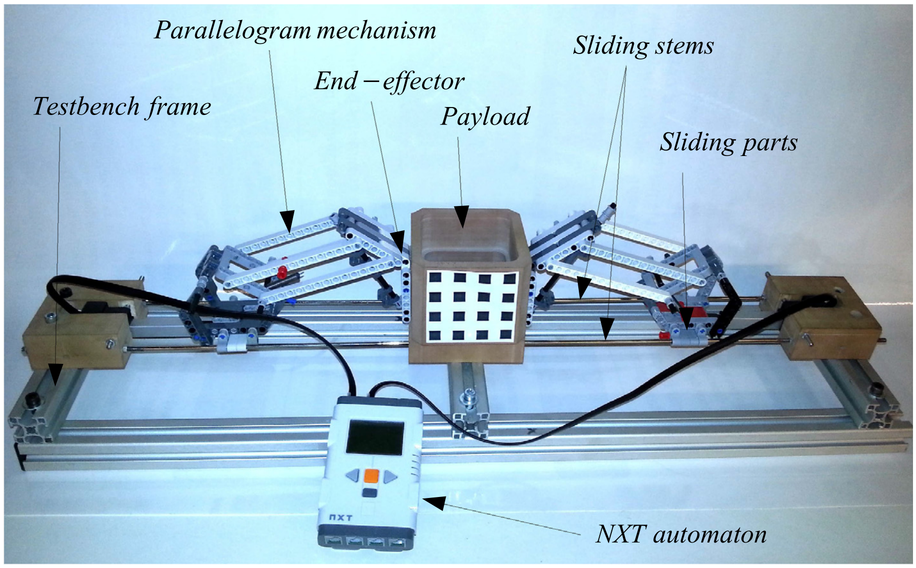

Fig. 13. Test-bench for lifting performances evaluation.

Table 3
Test-bench lifting results.

Type of contact	Type of actuation	Lift capacity
Rubber-rubber	Passive mechanism	0.6 kg
Rubber-rubber	Helical spring mechanism	0.82 kg
Rubber-composite	Passive mechanism	0.17 kg
Rubber-composite	Helical spring mechanism	0.5 kg
Plastic-composite	Passive mechanism	0.07 kg
Plastic-composite	Helical spring mechanism	0.18 kg

P-bot simulation using a manipulation mechanism with a diagonal helical spring . Fig. 10 presents the principle of simulation by including a helical extension spring between the points A and B of the parallelogram mechanism. Attaching the spring tips to the corners of the parallelogram instead of directly on one of the long bars has the advantage to introduce no additional bending in the bars.

Fig. 11 presents the simulation results for a payload co-manipulation using a helical extension springs with different stiffnesses. In the case of Fig. 11(a), the used spring generates a normal force relative to its deformation that allows the p-bot to maintain the payload catching and the overall system stability. The payload is put on robot bodies and the lifting phase is successfully achieved. The payload is able to slip when using a helical spring with a weak stiffness (Fig. 11(b)). However, Fig. 11(c) presents the simulation results using a higher stiffness spring that generates a normal force greater than the m-bot wheels propulsion which leads to the robots reversal. Using a helical spring, the system is able to lift in this case a payload with a mass around 0.4kg with two m-bots.

P-bot simulation using an interconnection mechanism. In this case it was considered that the robots end-effectors are connected to each other by a virtual system. Using an interconnection system allows to ensure the payload tightening during the different phases without loss of stability and without considering the risk of its slipping. The m-bots are able to lift the payload and put it on their top platform. The payload lifting capacity is limited to the applied pushing forces by the m-bots when the manipulation mechanism is not actuated. In the case where the parallelogram mechanism is actuated, the payload mass can reach the total weight of the used m-bots. In Fig. 12, the m-bots end-effectors and the payload have the same color as if they are a unique component and connected to each other. The simulation results have shown that, by

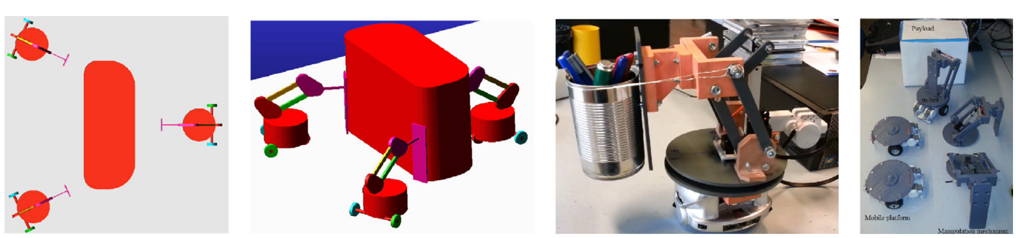

(a) Multi-body simulation (top View). (b) Multi-body simulation results (perspective View). (c) Manipulation mechanism mounted on a Khepera robot. (d) Prototype obtained with 3D printer.

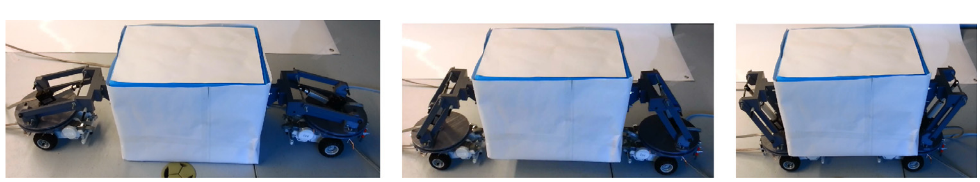

(e) Payload prehension (f) Payload lifting (g) Payload transport

Fig. 14. a, b) Multi-body 3D simulation; c, d) m-bot prototyping; e, f, g) payload co-lifting.

ensuring this interconnection and by actuating the lifting mechanism, the p-bot has considerable performances in terms of stability of the overall system and lifted payload weight. Two m-bot, of 1.4 kg each, can lift a payload of 3 kg.

4.2. Test-bench results

A test-bench was developed to validate the theoretical results using passive joints and spring actuation. The mechanism is made of a basis frame and two parallelogram systems mounted on two sliders actuated by horizontal linear actuators. This test-bench simulates the co-manipulation and lifting of a payload by two m-bots, without any risk of tip-over. The lifting capacities are evaluated according to various payload/end-effector friction coefficient. Fig. 13 presents the experimental mechanism and its components.

Two 6 V_{cc} Firgelli linear actuators with a maximal force of 23N were used to obtain the tangential forces applied by the wheels of two m-bots. The actuators are controlled by a unique Mindstorms NXT automaton in order to synchronize the forward motion of both lifting mechanism. The real pushing force is measured using a compression force sensor (Vernier Dual-Range Force Sensor DFS-BTA). The results where evaluated according to the lifting capacity using different contact materials in a passive way and with helical extension spring. Table 3 shows the obtained results.

According to experiments, the lifting capacity is higher while considering a higher friction coefficient (e.g., rubber-rubber contact is higher than plastic-composite contact). Experiments also proved that the use of compliant components improves the system efficiency in terms of manipulated payload since the deformed compliant organs will ensure a higher tightening force caused by the recalling forces.

4.3. 3D Simulations and manufactured prototypes results

Using ADAMS multi-body dynamic software, three robots were positiond around a payload to lift it using the proposed methodology. The results are shown in Fig. 14(a) and (b). Videos for simulation are visible under [25].

Two versions of prototypes were manufactured in order to validate the proposed strategy of co-manipulation and transport. Fig. 14(c) presents the first prototype of manipulation mechanism mounted on Khepera mobile robot and Fig. 14(d) presents the second prototypes tested for lifting and transport. The lifting and transport process by two m-bots is presented in Fig. 14(c)–(f).

The mechanism that ensures the co-lifting process is illustrated in Fig. 14(c)–(d) based on parallelogram structure that ensures a circular trajectory to lift the payload from the ground and put it on robots platform. Manufactured prototypes allow to experiment the proposed strategy of co-manipulation and co-transportation. The lifting and transport process by two m-bots is presented in Fig. 14(e)–(g) [25]. These developed systems will be used for future experiments and validation of the global strategy for co-manipulation and co-transportation proposed in this work.

The proposed co-manipulation strategy and transport were validated using the manufactured prototypes and the videos for experiments can be found in [25].

5. Conclusion and future work

This paper has presented the paradigm of our C^{3}Bots project (Collaborative Cross and Carry mobile roBots) which aims to co-manipulate, lift and transport any type of payload by a group of identical mobile manipulators with a simple architecture, called m-bots. The aggregation of several m-bots around the payload is named a p-bot. Its architecture is extremely modular, as the number and position of the m-bots can be adjusted according to the shape and mass of the payload. Each m-bot is mainly made of two parts: a mobile platform and a manipulation mechanism. A first implementation of this lifting mechanism has been presented. The developed p-bot is modular and can gather a variable number of m-bots to manipulate an object of a general shape. The m-bot was built from a single-axle robot (Khepera platform).The mechanism includes a passive vertical revolute joint that permits that each m-bot steers under the payload, thus allowing a global steering of the p-bot provided that all the axle axes converge to the same center of rotation. The mechanism also integrates a single DoF parallelogram mechanism that was designed to bring the payload from the ground to the upper platform of each m-bot by a circular trajectory, avoiding collision with the edge of the platform and maintaining the orientation of the payload during its lifting. The three cases of non-constrained, spring pre-constrained and actuated mechanism were considered for this parallelogram and it was shown that either a spring pre-constrained or an actuated mechanism could lift a payload. Adding an inter-connexion system between the end-effectors of all the m-bots can also substantially increase the lifting capacity of the p-bot. This preliminary design allows object manipulation without considering obstacle climbing which will be the goal of a second part of the project. For future work, experiments are under process for evaluating the transport efficiency with the p-bot. Stability will also have to be evaluated and optimized during prehension, lifting and transportation phases while taking into account objects shapes and weights. Additional compliance for the manipulation mechanism and a compliant end-effector for better contact with the payload surface will be studied and developed.

Acknowledgement

This work has been sponsored by the French government research program Investissements d'avenir through the IMobS3 Laboratory of Excellence LABEX (ANR-10-LABX-16-01), the RobotEx Equipment of Excellence (ANR-10-EQPX-44), and by the European Union through the program of Regional competitiveness and employment 2007-2013 (ERDF – Auvergne region).

References

[1] I.F. Vis, Survey of research in the design and control of automated guided vehicle systems, Eur. J. Oper. Res. 170 (3) (2006) 677–709.
[2] C. J-P, Elevateur pour mise en place des equipements de chantier.
[3] J.-Y. Wang, J.-S. Zhao, F.-L. Chu, Z.-J. Feng, Innovative design of the lifting mechanisms for forklift trucks, Mech. Mach. Theory 45 (12) (2010) 1892–1896.
[4] E. Mattar, A survey of bio-inspired robotics hands implementation: new directions in dexterous manipulation, Robot. Auton. Syst. 61 (5) (2013) 517–544.
[5] S.M. Hsiang, G.E. Brogmus, T.K. Courtney, Low back pain (lbp) and lifting technique:a review, Int. J. Ind. Ergon. 19 (1) (1997) 59–74.
[6] A. Plamondon, A. Delisle, S. Bellefeuille, D. Denis, D. Gagnon, C. Larivière, Lifting strategies of expert and novice workers during a repetitive palletizing task, Appl. Ergon. 45 (3) (2014) 471–481.
[7] R.R. Fox, J.L. Smith, A psychophysical study of high-frequency arm lifting, Int. J. Ind. Ergon. (2012).
[8] D. Rabinowitz, R. Bridger, M. Lambert, Lifting technique and abdominal belt usage: a biomechanical, physiological and subjective investigation, Saf. Sci. 28 (3) (1998) 155–164.
[9] Y. Aiyama, M. Hara, T. Yabuki, J. Ota, T. Arai, Cooperative transportation by two four-legged robots with implicit communication, Robot. Auton. Syst. 29 (1) (1999) 13–19.
[10] J.S. Bay, Design of the "army-ant" cooperative lifting robot, Robot. Autom. Mag. IEEE 2 (1) (1995) 36–43.
[11] F. Basile, F. Caccavale, P. Chiacchio, J. Coppola, C. Curatella, Task-oriented motion planning for multi-arm robotic systems, Robot. Comput. Integr. Manuf. 28 (5) (2012) 569–582.
[12] S. Liu, D. Sun, C. Zhu, A dynamic priority based path planning for cooperation of multiple mobile robots in formation forming, Robot. Comput. Integr. Manuf. 30 (6) (2014) 589–596.
[13] C. Schou, R.S. Andersen, D. Chrysostomou, S. Bøgh, O. Madsen, Skill-based instruction of collaborative robots in industrial settings, Robot. Comput. Integr. Manuf. 53 (2018) 72–80.
[14] M. Abou-Samah, V. Krovi, Optimal configuration selection for a cooperating system of mobile manipulators, ASME 2002 International Design Engineering Technical Conferences and Computers and Information in Engineering Conference, American Society of Mechanical Engineers, 2002, pp. 1299–1306.
[15] L. Adouane, L. Fort-Piat, Hybrid behavioral control architecture for the cooperation of minimalist mobile robots, Robotics and Automation, 2004. Proceedings. ICRA'04. 2004 IEEE International Conference on, 4 IEEE, 2004, pp. 3735–3740.
[16] M. Dorigo, D. Floreano, L.M. Gambardella, F. Mondada, S. Nolfi, T. Baaboura, M. Birattari, M. Bonani, M. Brambilla, A. Brutschy, et al., Swarmanoid, IEEE Robot.

Autom. Mag. 1070 (9932/13) (2013).
[17] O. Khatib, K. Yokoi, O. Brock, K. Chang, A. Casal, Robots in human environments: basic autonomous capabilities, Int. J. Robot. Res. 18 (7) (1999) 684–696.
[18] B.H. Wilcox, T. Litwin, J. Biesiadecki, J. Matthews, M. Heverly, J. Morrison, J. Townsend, N. Ahmad, A. Sirota, B. Cooper, Athlete: a cargo handling and manipulation robot for the moon, J. Field Robot. 24 (5) (2007) 421–434.
[19] T. Sugar, V. Kumar, Decentralized control of cooperating mobile manipulators, Robotics and Automation, 1998. Proceedings. 1998 IEEE International Conference on, 4 IEEE, 1998, pp. 2916–2921.
[20] H. Yamaguchi, M. Mori, A. Kawakami, Control of a five-axle, three-steering coupled-vehicle system and its experimental verification, World Congress, 18 (2011), pp. 12976–12984.
[21] B. Hichri, L. Adouane, J.-C. Fauroux, Y. Mezouar, I. Doroftei, Cooperative Mobile Robot Control Architecture for Lifting and Transportation of Any Shape Payload, Distributed Autonomous Robotic Systems, Springer, 2016, pp. 177–191.
[22] B. Hichri, L. Adouane, J.-C. Fauroux, Y. Mezouar, I. Doroftei, Flexible co-manipulation and transportation with mobile multi-robot system, Assembly Automation (2018).
[23] B. Hichri, J.C. Fauroux, L. Adouane, Y. Mezouar, I. Doroftei, Design of collaborative, cross & carry mobile robots" c^3bots", Adv. Mater. Res. 837 (2014) 588–593.
[24] B. Hichri, J.-C. Fauroux, L. Adouane, I. Doroftei, Y. Mezouar, Lifting Mechanism for Payload Transport by Collaborative Mobile Robots, New Trends in Mechanism and Machine Science, Springer, 2015, pp. 157–165.
[25] B. HICHRI, Simulation and experimental results for a group of mobile robots manipulating a payload, 2015, (https://www.dropbox.com/sh/0adqqudgvl2w1gp/AADsuTf5UzOSX-4J0XJZKiAaa?dl=0).